Landsat 9 Thermal Infrared Sensor 2 Pre-Launch Characterization: Initial Imaging and Spectral Performance Results

Aaron Pearlman[a], Joel McCorkel[b], Matthew Montanaro[c], Boryana Efremova[a], Brian Wenny[d], Allen Lunsford[e], Amy Simon[b], Jason Hair[b], and Dennis Reuter[b]

[a]GeoThinkTank LLC, Washington, DC, USA
[b]NASA Goddard Space Flight Center, Greenbelt, MD, USA
[c]Rochester Institute of Technology, Rochester, NY, USA
[d]Science Systems and Applications, Inc., Greenbelt, MD, USA
[e]Catholic University of America, Washington, DC, USA

ABSTRACT

The Thermal Infrared Sensor-2 (TIRS-2) aboard Landsat 9 will continue Landsat's four decade-long legacy of providing moderate resolution thermal imagery from low earth orbit (at 705 km) for environmental applications. Like the Thermal Infrared Sensor aboard Landsat 8, it is a pushbroom sensor with a cross-track field of view of 15° and provides two spectral channels at 10.8 and 12 μm. To ensure radiometric, spatial, and spectral performance, a comprehensive pre-launch testing program is being conducted at NASA Goddard Space Flight Center at the component, subsystem, and instrument level. This paper will focus on the results from the subsystem level testing where the instrument is almost completely assembled. This phase of testing is specifically designed to assess imaging performance including focus and stray light rejection, but is also used to provide a preliminary assessments of spatial and spectral performance. The calibration ground support equipment provides a flexible blackbody illumination source and optics to conduct these tests. The spectral response test setup has its own illumination source outside the chamber that propagates through the calibration ground support equipment in an optical configuration designed for this purpose. This test configuration with the calibration ground support equipment and TIRS-2 subsystem in the thermal vacuum chamber enables a large range of illumination angles for stray light measurements. The results show that TIRS-2 performance is expected to meet all of its performance requirements with few waivers and deviations.

Keywords: Thermal Infrared Sensor 2, Landsat 9, pre-launch calibration, imaging, spectral, spatial

1. INTRODUCTION

The Thermal Infrared Sensor-2 (TIRS-2) aboard Landsat 9, a follow-on to TIRS on Landsat 8, is scheduled to launch at the end of 2020 to continue the Landsat Program's legacy of providing moderate resolution thermal imagery [1, 2, 3]. Scientists use the imagery for a wide variety of environmental applications like assessing evapotranspiration through land surface temperature retrievals. The two bands, at 10.8 μm and 12 μm, enable more accurate retrievals by using split window techniques than using the single channel available prior to Landsat 8 [4].

The instrument is a pushbroom sensor with a 15° cross-track field of view with the same basic architecture as TIRS but has some improvements such as increased redundancy to meet higher reliability requirements. It has a f/1.6 four-lens telescope that focuses onto quantum well infrared detector (QWIP) arrays, an on-board blackbody for calibration, and a scene-select mirror for switching between Earth view, blackbody, and space views. It is also designed for improved stray light rejection to address one of the key performance issues found on TIRS [5, 6]. Added baffles are meant to block the major stray light paths from 13° and 22° off axis to mitigate

Further author information: (Send correspondence to A.Pearlman)
A.Pearlman: E-mail: aaron@geothinktank.com or aaron.j.pearlman@nasa.gov, Telephone: 1 301 286 3956

this issue. Each of three QWIP detector arrays or sensor chip arrays (SCAs), together called the focal plane array (FPA), is operated at ∼40 K and consists of a 512 row x 640 column array with a filter covering 30 pixel rows for each channel with a completely opaque section in-between [7]. Two science rows out of the 30 will be used as operational rows such that the combination from all science rows will cover 1850 pixel columns to form a 185 km swath.

The TIRS-2 team at NASA Goddard Space Flight Center, formed in 2015, is fabricating and testing the instrument and is on track for a August 2019 delivery to the spacecraft [8]. Pre-launch testing is done at component, subsystem, and instrument-level to ensure radiometric, spatial, and spectral performance. We report here on the phase of testing called TIRS-2 Imaging Performance and Cryoshell Evaluation (TIPCE), which occurred in the November 2017 to March 2018 time frame. TIPCE tests the TIRS-2 assembly consisting of the flight telescope, FPA, and FPA electronics but without the scene select mirror. The aperture of the scene select mirror is simulated with the a front end baffle simulator. One of the key objectives of the initial pre-launch testing was to characterize the residual stray light. The other main objective was to determine and verify the focus position of the focal plane arrays (FPA) with respect to the telescope. This drives the spatial response performance, so an additional test is performed with the instrument in-focus to obtain an initial spatial performance estimate. A spectral response test provides preliminary data to compare to requirements and component-level measurements.

To perform these tests, the TIRS-2 assembly is placed in a thermal vacuum chamber across from the calibration ground support equipment (GSE) consisting of a blackbody on a translation stage with a target wheel containing a selection of apertures for projecting onto the TIRS-2 FPA Fig.1. The blackbody light is collimated with an off-axis parabolic mirror (OAP) and directed with the steering mirror that can translate and rotate both in the azimuth and elevation directions. The calibration GSE configuration shown is used for all tests except for the spectral response test (discussed later). An additional blackbody closer to the TIRS-2 assembly is not used for this test but will be available for radiometric testing.

2. FOCUS TEST

2.1 Methodology

The TIRS-2 FPA focus is measured to ensure that the FPA lies at the optimal position relative to the telescope. If the focus needs to change, shims are fabricated to move the FPA position relative to the telescope. After shims are changed, the focus is then verified to ensure that the shims were fabricated and installed correctly. The focus test involves sweeping the focal position through a range of values, and at each position, a two pixel-sized blackbody image is projected onto various positions on the focal plane. Each image is fit with a Gaussian-based model and the full-width-half maximum (FWHM) is calculated to find the position with the lowest FWHM value corresponding to the maximum focus. Instead of moving the TIRS-2 FPA position directly, the blackbody is moved instead to change the beam focus. This distance in object space is converted to image or FPA space.

2.2 Results

The initial focus test with the flight FPA (TIPCE-2) demonstrated the need for shim adjustments. The shims were installed and the focus test was repeated (TIPCE-3). The results show that the FPA is in focus (Fig 2). The figure displays a map with maximum focus blackbody position along the arrays. These values correspond to negligible shim thickness changes of less than 8 μm (= 0.0003 inches). Note that the telescope temperature can be controlled to change the focus as well, though based on these results, temperature adjustment was deemed unnecessary. This test will be repeated for instrument-level testing to confirm the results with the scene select mirror.

3. SPATIAL RESPONSE TEST

3.1 Methodology

The methodology follows the same one used for TIRS [9]. The spatial response is characterized in terms of the edge response function at various TIRS-2 FPA locations. A square target initially planned for TIRS pre-launch testing seemed to suffer from a vignetting issue, so an edge from a 16-pixel circle target was used instead.

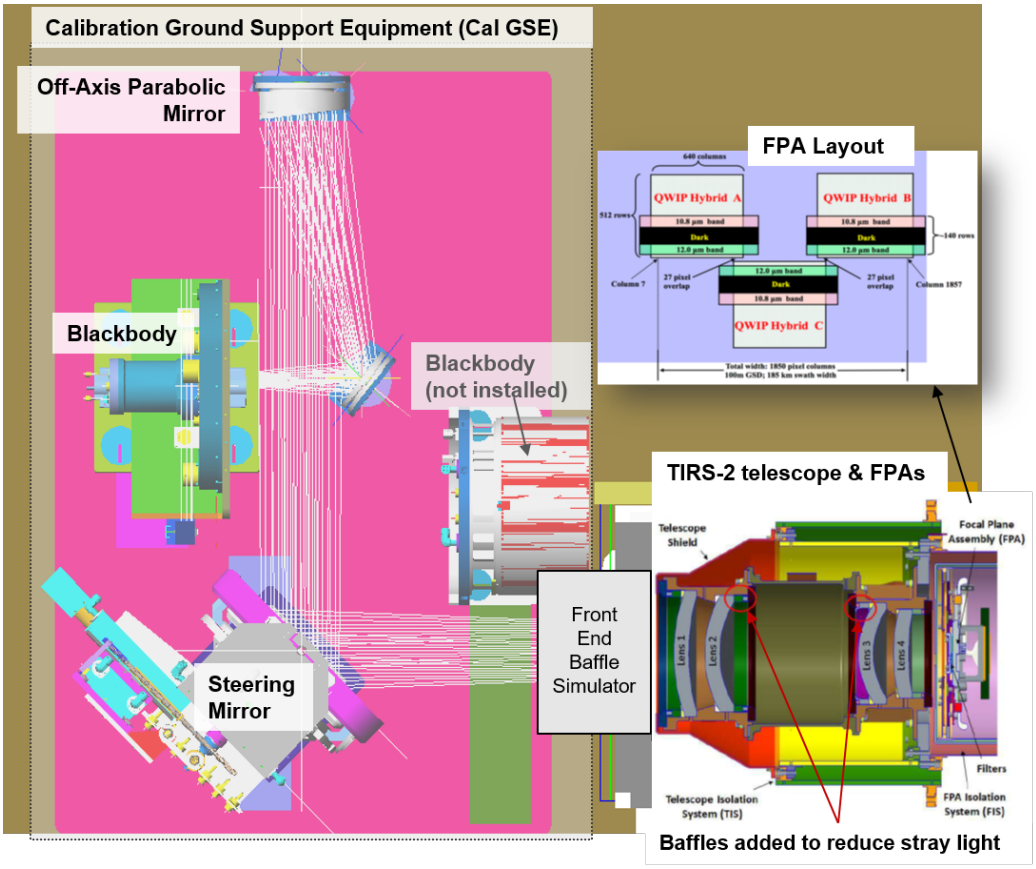

Figure 1. Configuration for focus, stray light, and spatial response testing including the Calibration Ground Support Equipment and the TIRS-2 telescope and focal plane arrays (FPAs). The added baffles for stray light mitigaton are illustrated along with the FPA layout.

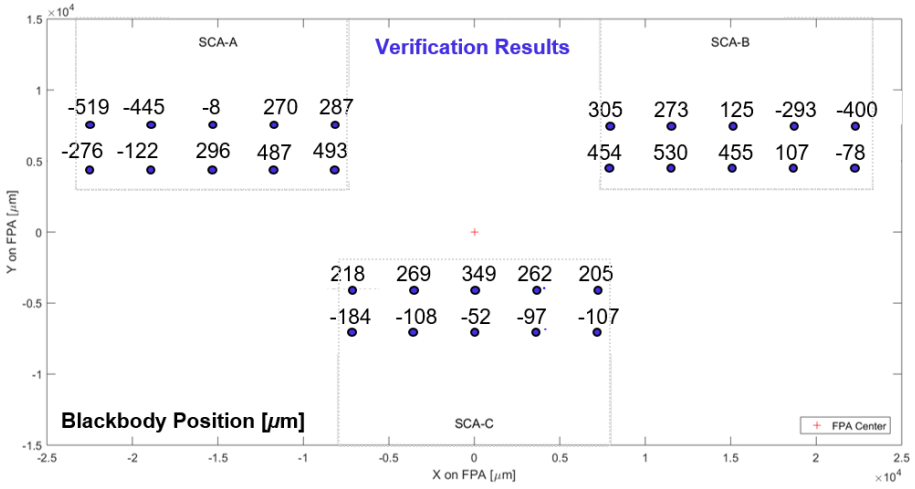

Figure 2. Map of FPA layout with overlaid maximum focus blackbody positions along the arrays

The target is moved in sub-pixel steps in either the along-tack or cross-track direction. The FPA frames are background subtracted and flat-fielded and their central cross-section is adjusted so that the edges are aligned to form a well-populated edge spread function (Fig. 3). The TIRS-2 requirements are compared to the derived edge slope and edge extent.

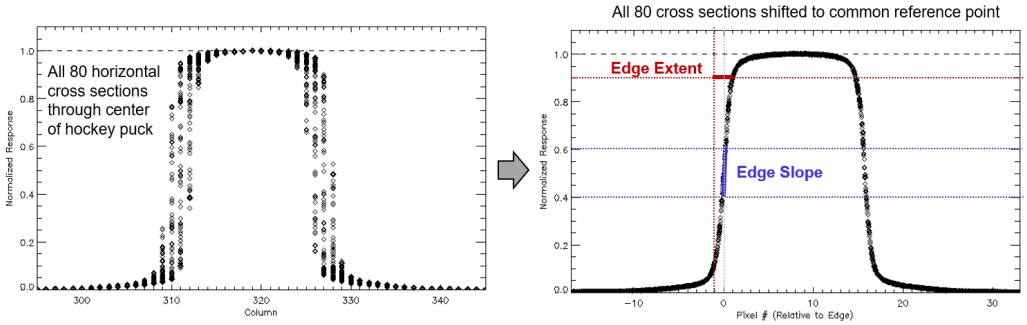

Figure 3. An example of a horizontal cross sections of the center of the 16-pixel diameter target during the spatial response test aligned to derive the edge response and edge slope.

3.2 Results

The edge slope and edge extent results are shown in Fig. 4 and 5, respectively. In the figure, the SCAs are combined so that SCA-A = column #1-640, SCA-B = column #641-1280), and SCA-C = column #1281-1920. (Note that this exceeds the 1850 pixels used in operations because of overlapping regions among the SCAs). They show the consistency between repeated tests (TIPCE-2 and TIPCE-3), consistency across the arrays, and a strong indication that the requirements will be met for both channels at instrument-level testing. The edge slope and edge extent are similar to those obtained during TIRS pre-launch testing (Table 1) [9] suggesting that TIRS-2 will have similar spatial performance to TIRS. This test will be repeated at instrument-level thermal vacuum testing to include the impact of the scene select mirror.

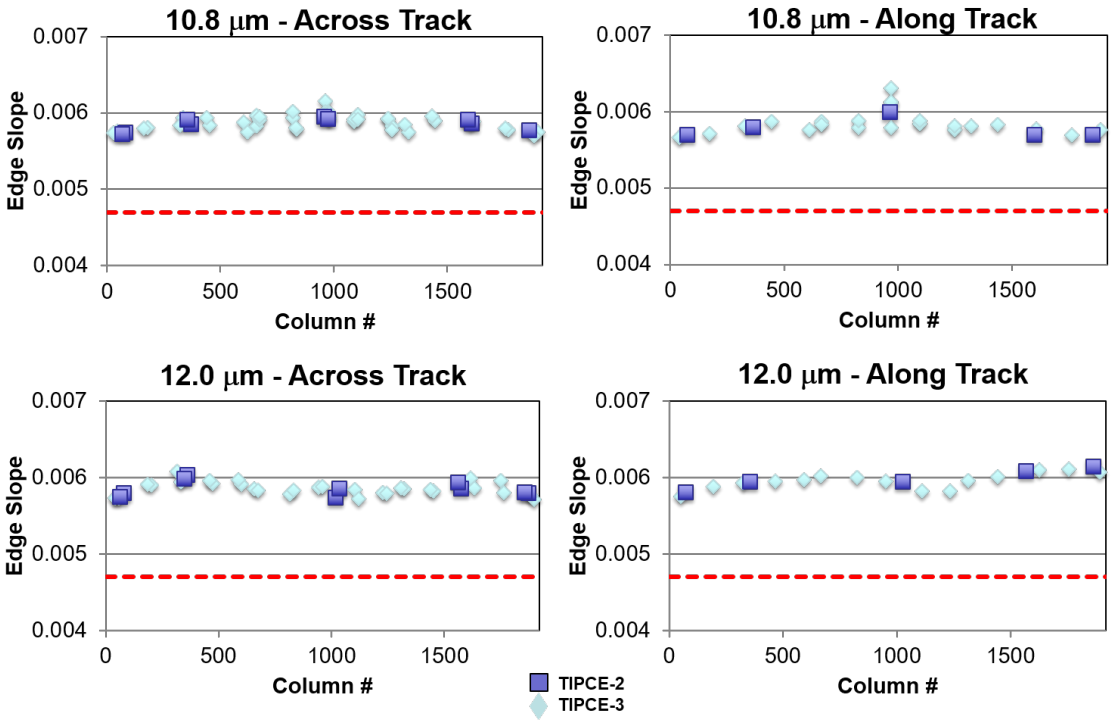

Figure 4. Edge slope results for the 10.8 and 12.0 μm channels in the along and cross-track directions relative to the requirement (dotted red line).

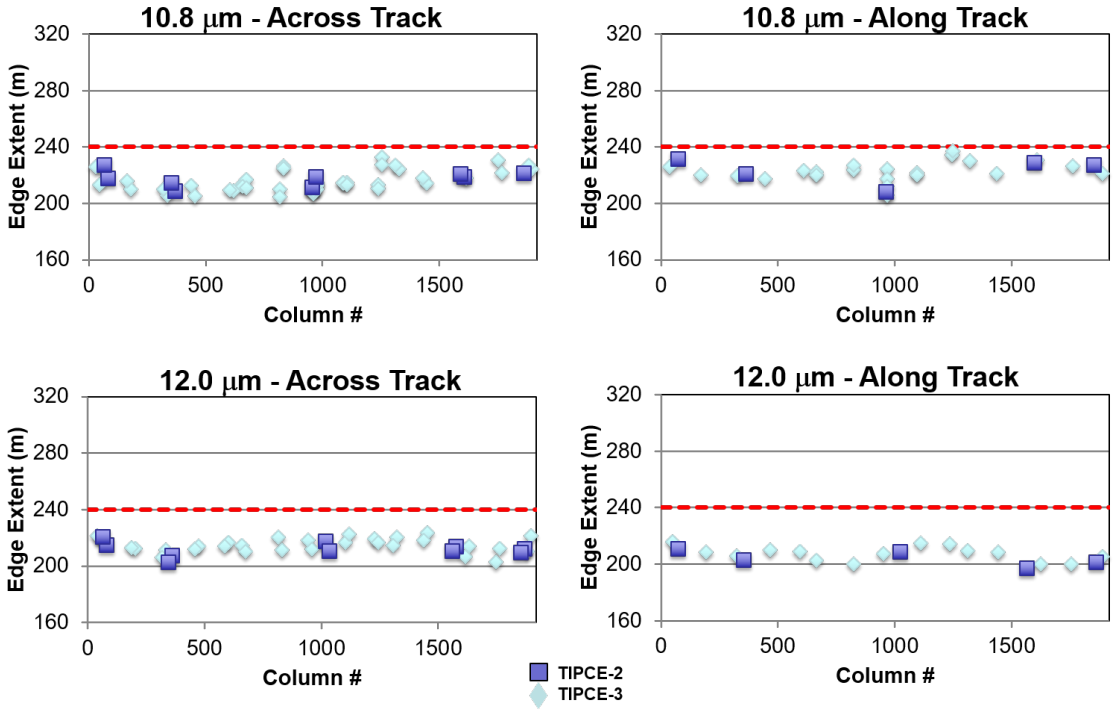

Figure 5. Edge extent results for the 10.8 and 12.0 μm channels in the along and cross-track directions relative to the requirement (dotted red line).

Table 1. Comparison between TIRS2 and TIRS pre-launch measurements

	Channel	Direction	TIRS-2 (TIPCE-3) Mean	TIRS-2 (TIPCE-3) σ	TIRS Pre-launch Mean	TIRS Pre-launch σ
Edge Slope (pixel^{-1})	10.8 µm	Cross	0.0059	0.0001	0.0059	0.0002
	10.8 µm	Along	0.0058	0.0002	0.0053	0.0003
	12.0 µm	Cross	0.0059	0.0001	0.0061	0.0001
	12.0 µm	Along	0.0060	0.0001	0.0063	0.0002
Edge Extent (m)	10.8 µm	Cross	215.6	7.3	202.8	9.1
	10.8 µm	Along	222.8	6.8	234.0	17.1
	12.0 µm	Cross	214.9	5.1	197.6	6.9
	12.0 µm	Along	207.5	5.2	184.3	11

4. SCATTER SURVEY TEST

4.1 Methodology

The scatter survey test is designed to characterize stray light over a large range of angles including the expected residual stray light from 22° and 13° off-axis. The full range of angles available in the configuration is due to the absence of the scene select mirror (not yet integrated) and adjustments made to the steering mirror to maximize its range (Fig 6a). Optical modeling is used in conjunction with this test to extend the results to areas outside of this range. Each dot in the figure represents a location where a 0.7°-square target is projected using a blackbody set to 500 K – above the nominal value of 360 K used for other tests. In order to detect small signals, we also use the largest available integration time 5.5 ms and define 100% signal as the response to a 500 K blackbody at that integration time. Because this signal saturates the detectors upon direct illumination, we sweep the integration times and extrapolate to find the unsaturated value later used for scaling the results to percent signal. At each location, all detectors are read out and evaluated for stray light signal.

4.2 Results

The red squares in Fig. 6a show all locations where any signal was detected on the FPA. The near on-axis positions were excluded to emphasize the far off-axis scattered signal (Those are evaluated separately). The feature near 22° is broader but lower in signal compared to the brighter but narrower 13° feature. The quantitative results are shown in percent signal summed from all measured locations in Fig. 6b. SCA-B shows the largest signal at about 0.35% while others are substantially lower. The stray light from the entire off axis area was determined with the aid of optical modeling. By taking the ratio between the modeled stray light signal summed from the entire area to the modeled stray light sum from the measured area and multiplying by the measured stray light sum, we obtain the total stray light. This is summarized in the table showing a worst case estimate of 0.76% and 1.11%, for the 10.8 μm and 12 μm channels, respectively. This is about a factor of 7-8 improvement over TIRS-1 performance [6]. Further evaluation is underway to refine optical modeling results and science data product impacts [10].

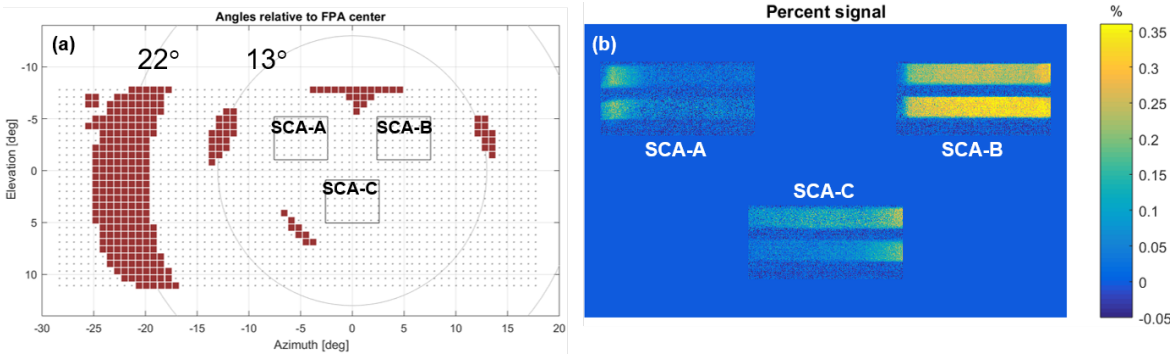

Figure 6. Scatter survey test results (a) The red squares show locations where any stray light signal was detected. The red dots show all measured locations. (b) The sum of all stray light signals on the FPAs over the entire measured area expressed in percent signal.

Table 2. Scatter results scaled with an optical model

	10.8 μm Channel	12.0 μm Channel
SCA-A	0.69%	1.11%
SCA-B	0.76%	1.01%
SCA-C	0.24%	0.21%

5. SPECTRAL RESPONSE TEST

5.1 Methodology

The spectral response is measured using an alternate path through the calibration GSE specifically designed for this test (Fig. 7). A monochromator-based setup with a 1000 K blackbody illuminates the monochromator with 2 mm-wide slits (150 nm dispersion). The output is collimated with a 6"-focal length OAP and through the chamber window to the calibration GSE, where the beam is focused, re-collimated, and projected onto various regions of the TIRS-2 FPA. The regions are selected to sample different (normalized) quantum efficiency regions to see if these relate to spectral uniformity. A liquid nitrogen-cooled HgCdTe detector with a known spectral response serves as a reference detector (with signal V_{ref}). Spectral measurements involve incrementing the monochromator wavelength in steps of 50 nm over each channel while taking either TIRS-2 measurements or reference detector measurements. The reference and TIRS-2 spectral measurements are taken sequentially. The difference in the spectral transmittance (τ) between the reference path ($ref\,path$) and TIRS-2 path is taken into account to derive the spectral response:

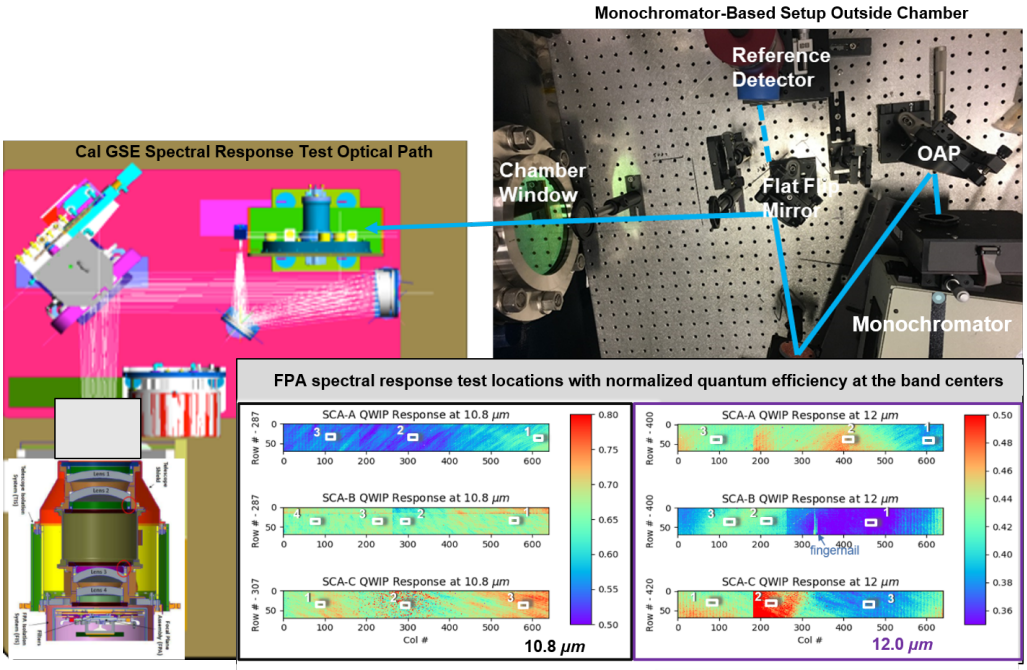

Figure 7. The spectral response test setup showing the monochromator-based setup outside the thermal vacuum chamber and the alternate path through the calibration GSE used for this test. The FPA locations were sampled to sample different detector responsivity behavior as shown.

$$dn_{corr}(\lambda, pix) = \frac{dn_{TIRS}(\lambda, pix) \times \tau_{ref\ path}}{\tau_{TIRS\ path} \times V_{ref}} \tag{1}$$

The relative spectral response is then $RSR = \frac{dn_{corr}(\lambda,pix)}{max(dn_{corr}(\lambda,pix))}$.

5.2 Results

The spectral response functions for all measured locations within each SCA and channel show consistent results within each channel/SCA (Fig. 8) though some differences in shape exist for the different SCAs for each channel. Fig. 9 shows consistency in central wavelength and band edges across all the detectors (dark blue dots) for both channels, and that they are expected to meet the associated requirements (red dotted lines). Fig. 10 shows that the results meet the spectral uniformity requirements for central wavelength and FWHM and did not reveal a clear dependence on quantum efficiency. These results are also compared with component-level measurements conducted at the NASA Detector Characterization Lab as a preliminary validation of the results. Detector-filter combination spectral measurements were taken at several angles without the TIRS-2 f/1.6 telescope. The spectral response at different angles (σ) were used to derive an equivalent f/1.6 spectral response using a weighted sum according to their solid angles:

$$RSR_{f/1.6} = \sum_i \frac{RSR(\sigma_i) sin(\sigma_i) \Delta\sigma_i}{1 - cos(\sigma_{max})} \tag{2}$$

The metrics with these derived spectral responses, shown in light blue or orange in Figs. 9-10, agree reasonably well with the TIPCE results [11]. In general, the 10.8 μm agreement for all metrics is slightly better than for channel 12.0 μm channel. The shading in the component-level measurements are uncertainty estimates based on the difference between two different measurement setups. Other sources of uncertainty such as the f/1.6 adjustment uncertainty is not included here. The TIPCE spectral response setup is being refined for instrument-level testing and is expected to have lower and more-easily-quantifiable uncertainties.

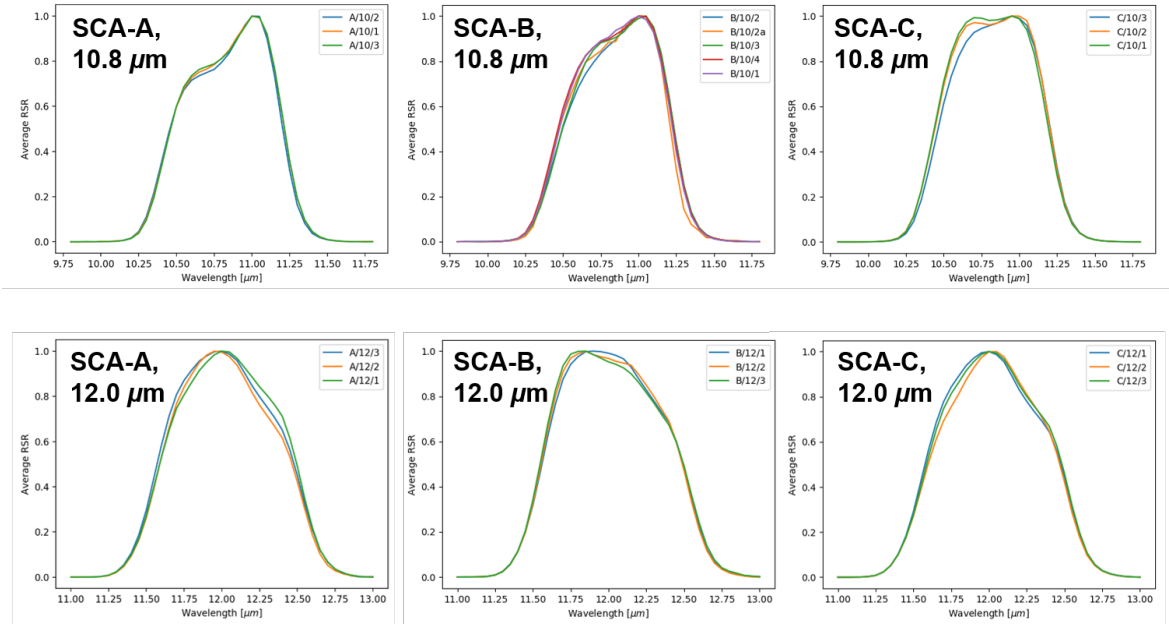

Figure 8. The spectral response functions for all measured locations for each SCA and channel.

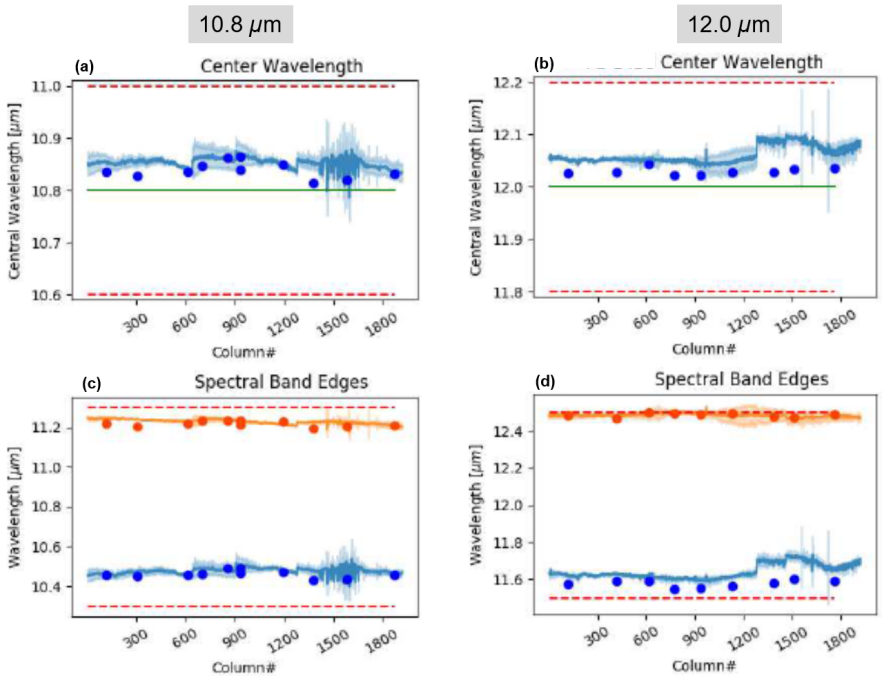

Figure 9. The spectral response function central wavelength and FWHM derived for each SCA for all measured locations. The SCAs are combined so that SCA-A = column #1-640, SCA-B = column #641-1280), and SCA-C = column #1281-1920. The blue dots represent TIPCE results, the light blue or orange line represents the adjusted component-level results with shading to represent the estimated uncertainty, and the red lines shows the requirements.

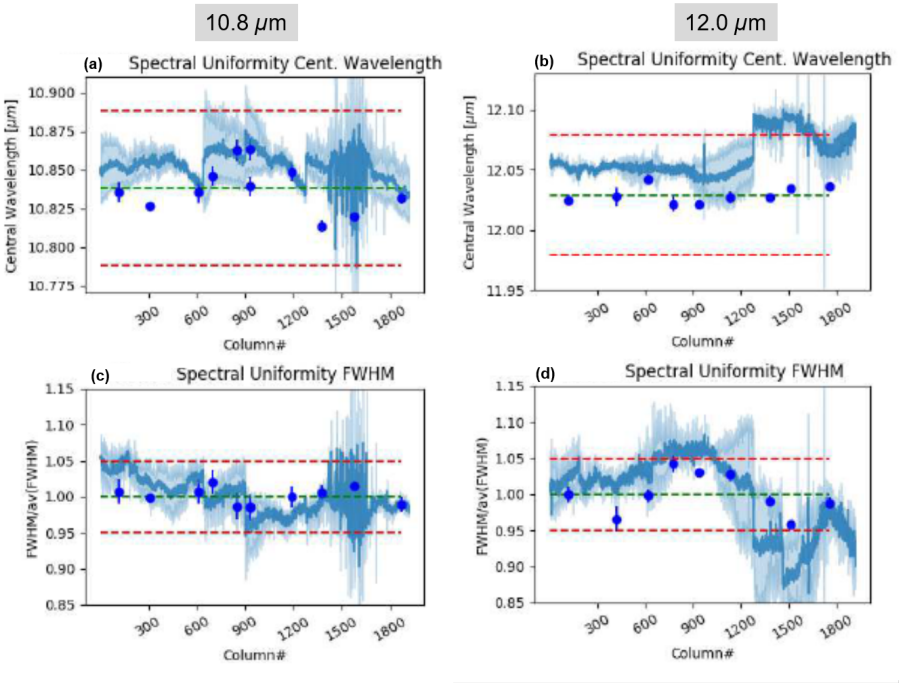

Figure 10. The uniformity of the central wavelength and FWHM derived for each SCA for all measured locations. The SCAs are combined so that SCA-A = column #1-640, SCA-B = column #641-1280), and SCA-C = column #1281-1920. The blue dots represent TIPCE results, the light blue line represents the adjusted component-level results with shading to represent the estimated uncertainty, and the red lines shows the requirements.

5.3 Conclusion

The initial pre-launch TIRS-2 performance results show that TIRS-2 is expected to meet all of its performance requirements with few waivers and deviations. The focus was set and verified, and spatial and spectral response of the instrument assembly were measured as a preliminary characterization. The TIRS-2 spatial response results show similar spatial performance to TIRS. The spectral results show good agreement with component-level measurements accounting for the angular dependence of the detector spectral response. The scatter survey showed improved stray light rejection compared to TIRS with the total stray light effect of 1% or less. Current preparations for instrument-level thermal vacuum testing are now underway where a comprehensive set of tests – including another set of focus, scatter, spatial response, and spectral response tests – will be conducted. The TIRS-2 team is on track to deliver a well-characterized instrument that will meet data users' needs for a variety of environmental applications.

ACKNOWLEDGMENTS

The authors acknowledge the critical support of the TIRS-2 team at Goddard Space Flight Center. In particular, we thank Dr. June Tveekrem for optical modeling support, Jeff Love for software support, and Justin Bird and Josh Felt for calibration GSE hardware/software support.

References

[1] Reuter, D. C., Richardson, C. M., Pellerano, F. A., Irons, J. R., Allen, R. G., Anderson, M., Jhabvala, M. D., Lunsford, A. W., Montanaro, M., Smith, R. L., Tesfaye, Z., and Thome, K. J., "The Thermal Infrared Sensor (TIRS) on Landsat 8: Design overview and pre-launch characterization," *Remote Sensing* **7**(1), 1135–1153 (2015).

[2] Irons, J. R., Dwyer, J. L., and Barsi, J. A., "The next Landsat satellite: The Landsat data continuity mission," *Remote Sensing of Environment* **122**, 11 – 21 (2012). Landsat Legacy Special Issue.

[3] Hair, J. H., Reuter, D., Tonn, S. L., McCorkel, J., Simon, A. A., Djam, M., Alexander, D., Ballou, K., Barclay, R., Coulter, P., Edick, M., Efremova, B., Finneran, P., Florez, J., Graham, S., Harbert, K., Hewitt, D., Hickey, M., Hicks, S., Hoge, W., Jhabvala, M., Lilly, C., Lunsford, A., Mann, L., Masters, C., Montanaro, M., Muench, T., Otero, V., Parong, F., Pearlman, A., Penn, J., Vigneau, D., and Wenny, B., "Landsat 9 Thermal Infrared Sensor 2 architecture and design," in [*Proceedings of IEEE International Geoscience & Remote Sensing Symposium*], (2018). Manuscript submitted for publication.

[4] Yu, X., Guo, X., and Wu, Z., "Land surface temperature retrieval from Landsat 8 TIRS—comparison between radiative transfer equation-based method, split window algorithm and single channel method," *Remote Sensing* **6**(10), 9829–9852 (2014).

[5] Montanaro, M., Gerace, A., Lunsford, A., and Reuter, D., "Stray light artifacts in imagery from the Landsat 8 Thermal Infrared Sensor," *Remote Sensing* **6**(11), 10435–10456 (2014).

[6] Gerace, A. and Montanaro, M., "Derivation and validation of the stray light correction algorithm for the Thermal Infrared Sensor onboard Landsat 8," *Remote Sensing of Environment* **191**, 246 – 257 (2017).

[7] Jhabvala, M., Reuter, D., Choi, K., Jhabvala, C., and Sundaram, M., "QWIP-based Thermal Infrared Sensor for the Landsat data continuity mission," *Infrared Physics & Technology* **52**(6), 424 – 429 (2009). Proceedings of the International Conference on Quantum Structure Infrared Photodetectors (QSIP) 2009.

[8] McCorkel, J., Montanaro, M., Efremova, B., Pearlman, A., Wenny, B., Lunsford, A., Simon, A. A., Hair, J., and Reuter, D., "Landsat 9 Thermal Infrared Sensor 2 characterization plan overview," in [*Proceedings of IEEE International Geoscience & Remote Sensing Symposium*], (2018). Manuscript submitted for publication.

[9] Wenny, B. N., Helder, D., Hong, J., Leigh, L., Thome, K. J., and Reuter, D., "Pre- and post-launch spatial quality of the Landsat 8 Thermal Infrared Sensor," *Remote Sensing* **7**(2), 1962–1980 (2015).

[10] Montanaro, M., McCorkel, J., Tveekrem, J., Stauder, J., Lunsford, A., Mentzell, E., Hair, J., and Reuter, D., "Landsat 9 Thermal Infrared Sensor 2 preliminary stray light assessment," in [*Proceedings of IEEE International Geoscience & Remote Sensing Symposium*], (2018). Manuscript submitted for publication.

[11] Efremova, B., Pearlman, A., Mccorkel, J., Montanaro, M., Hickey, M., Lunsford, A., and Reuter, D., "Landsat 9 Thermal Infrared Sensor 2 subsystem-level spectral test results," in [*Proceedings of IEEE nternational Geoscience & Remote Sensing Symposium*], (2018). Manuscript submitted for publication.